# Computational Astrophysics Report

Anandhu Anilkumar Binu, Laraib Mustafa Mirza

February 20, 2026

**Abstract**

Using an N-body simulation, we studied the dynamical evolution of a stellar population within a Milky Way-like potential. We simulate the orbits of $10^4$ high-mass stars, focusing on the post-supernova phase and the resulting dynamics of neutron stars and black holes. Our methodology combines 'sevnpy' for stellar evolution and 'fireworks' for N-body dynamics, allowing us to model the gravitational potential of the Milky Way and integrate the orbits of stars over time. We explore the impact of different supernova kick models and metallicities on the final spatial distribution of neutron stars and black holes. Our findings reveal that neutron stars experience more significant displacements due to supernova kicks than black holes, resulting in a broader radial and vertical distribution. This provides insights into the dynamical processes affecting stellar remnants and their role in shaping the galaxy's structure.

## 1 Introduction

Many astrophysical objects experience a velocity kick during their evolution. The most notable case is that of neutron stars, particularly pulsars, which have significantly higher space velocities than their progenitors, indicating they received an additional velocity—a natal kick—at birth [6, 11, 17]. It is well established that neutron stars (NSs) receive natal kicks in the range of $\sim$ 200–400 km $s^{-1}$ when they are formed in core-collapse supernovae (SNe) [7, 17].Other instances of likely kicks include stellar-mass black holes [1, 9, 15, 18, 22] and binary systems, which receive a systemic kick due to mass loss after one of the components undergoes a supernova [2, 4, 5, 8, 10, 13, 23, 24, 25, 26]. The velocity distribution of kicked objects evolves and varies with the Galactic location where it is measured.

The question of whether stellar-mass black holes receive natal kicks is still open. These black holes can be studied through interacting X-ray binaries. Several known X-ray binaries contain black holes or black hole candidates [15, 21]. In these systems, a massive primary evolves into a black hole via a core-collapse SN, and material from a lower mass secondary accretes onto the black hole, typically through Roche lobe overflow. When the primary undergoes a supernova, the resulting mass loss can unbind the binary or impart a kick to the system due to the net momentum change in the binary's rest frame. Any natal kick received by the black hole will affect the orbital properties of the binary and its motion within the Galaxy.By studying the orbits and locations of stars and binaries within the Galaxy, we can understand how velocity kicks influence Galactic evolution over time. In this study, we simulate the evolution of $10^4$ high-mass stars in thin-disc orbits within the Milky Way, focusing on the post-supernova phase and the resulting dynamics of neutron stars and black holes. We integrate the orbits of these stars and their remnants over 5 Gyr post-supernova kick and analyze their spatial distribution; section 2 describes our methodology to model the Milky Way's gravitational potential and generate the stellar population. We outline the stellar evolution simulation using the SEVN [14] package and the orbit integration process,

Section 3 details the spatial analysis performed on the simulation results.

# 2 Methodology

## 2.1 N-body Simulation

N-body simulations are a computational technique used to model gravitational interactions among multiple bodies over time. Using an N-body simulation, we simulated the dynamical evolution of a stellar population within a Milky Way-like potential. We initialized a stellar population with positions and circular velocities appropriate for a disc galaxy, employing the Kroupa Initial Mass Function (IMF) for stellar masses. SEVN [14] was employed to create star objects with initial masses and metallicities, evolve these stars over time, and handle supernova events by retrieving the resulting kick velocities and remnant types. Meanwhile, fireworks were utilized for unit conversions and scaling, defining various potential models and combining these into a composite potential. The library managed particle data, including positions, velocities, and masses, and calculated gravitational accelerations on these particles. The symplectic leapfrog integrator numerically integrated the equations of motion, ensuring energy conservation over long periods. This integrator was used to evolve the stars' orbits over time, while stellar evolution using SEVN updated masses and velocities based on events like supernovae. After the simulation, the code identified the final positions of neutron stars and black holes. The outcomes were recorded, capturing the initial and final positions of stellar remnants for analysis. Combining SEVN for stellar evolution and fireworks for N-body dynamics, this comprehensive simulation framework effectively studied a stellar population's dynamic and evolutionary processes in a galaxy-like environment.

We generated a gravitational potential and integrated the orbits. In this potential, we generated a stellar population with masses ranging from $10M_\odot$ to $150M_\odot$, ensuring that the remnants would be either neutron stars or black holes. Each member of this stellar population further evolved until they reached the supernova stage. We added the velocity kick imparted to the orbit during the supernova event. After the supernova, we continued the orbit integration to observe how the orbits evolved for 5 Gyr.

## 2.2 Gravitational Potential

The gravitational potential of the Milky Way was described using a multi-component potential incorporating three widely used analytical components: the Navarro-Frenk-White (NFW) halo potential, the Miyamoto-Nagai disc potential, and the Truncated Power-Law bulge potential. These components were combined into a single class, `MilkyWayPotential`, which provides combined particle acceleration in the potential field.

- **Navarro-Frenk-White (NFW) Halo Potential:** The NFW profile is a standard model for dark matter halos, introduced by Navarro, Frenk, and White [20]. The density profile is given by:

$$\rho(r) = \frac{\rho_0}{\left(\frac{r}{r_s}\right)\left(1+\frac{r}{r_s}\right)^2} \tag{1}$$

  where $\rho_0$ is a characteristic density and $r_s$ is the scale radius. The corresponding gravitational potential is:

$$\Phi_{\rm NFW}(r) = -\frac{GM_{\rm vir}}{r}\ln\left(1+\frac{r}{r_s}\right) \tag{2}$$

  where $M_{\rm vir} = 0.8\times10^{12}\,M_\odot$ is the virial mass of the halo, and $r_s = 16\,\mathrm{kpc}$ is the scale radius.

- **Myamoto-Nagai Disc Potential:** The Myamoto-Nagai potential is widely used to model the galactic disc, as presented by Miyamoto and Nagai [19]. The potential is given by:

$$\Phi_{\rm MN}(R,z) = -\frac{GM_{\rm disc}}{\sqrt{R^2+\left(a+\sqrt{z^2+b^2}\right)^2}} \tag{3}$$

  where $R$ is the radial distance in the plane of the disc, $z$ is the vertical distance above or below the

plane, $a = 3\,\text{kpc}$ and $b = 0.28\,\text{kpc}$ are scale parameters of the disc, and $M_{\text{disc}} = 6.8 \times 10^{10}\, M_\odot$ is the mass of the disc.

- **Truncated Power-Law Bulge Potential:** The Truncated Power-Law model for the bulge is based on a generalized model often attributed to Hernquist [12]. The density profile is given by:

$$\rho(r) = \frac{\rho_0}{\left(1 + \frac{r}{r_a}\right)^{\gamma}} \left(1 + \left(\frac{r}{r_t}\right)^{\alpha}\right)^{-1} \tag{4}$$

where $\rho_0$ is a characteristic density, $r_a = 1\,\text{kpc}$ is the scale radius, $\gamma = 1.8$ is the power-law slope, $r_t = 1.9\,\text{kpc}$ is the truncation radius, and $\alpha$ is the truncation slope. The corresponding gravitational potential is:

$$\Phi_{\text{TPL}}(r) = -\frac{GM_{\text{spher}}}{\left(1 + \frac{r}{r_a}\right)^{\gamma}} \left(1 + \left(\frac{r}{r_t}\right)^{-\alpha}\right)^{-1} \tag{5}$$

where $M_{\text{spher}} = 0.5 \times 10^{10}\, M_\odot$ is the mass of the bulge.

The combined potential allows for calculating the acceleration on a particle within the Milky Way potential. The total acceleration $\mathbf{a}$ experienced by a particle at position $\mathbf{r}$ is given by the sum of the accelerations due to each component:

$$\mathbf{a}(\mathbf{r}) = \mathbf{a}_{\text{NFW}}(\mathbf{r}) + \mathbf{a}_{\text{MN}}(\mathbf{r}) + \mathbf{a}_{\text{TPL}}(\mathbf{r}) \tag{6}$$

where:

$$\mathbf{a}_{\text{NFW}}(\mathbf{r}) = -\frac{GM_{\text{vir}}}{r^2} \left(\ln\left(1 + \frac{r}{r_s}\right) - \frac{r}{r_s + r}\right) \hat{\mathbf{r}}$$

$$\mathbf{a}_{\text{MN}}(\mathbf{r}) = -\nabla \Phi_{\text{MN}}(R, z)$$

$$\mathbf{a}_{\text{TPL}}(\mathbf{r}) = -\nabla \Phi_{\text{TPL}}(r)$$

## 2.3 Stellar Population Initialization

The stellar population is generated using a function that assigns positions, velocities, and masses to a specified number of stars. The spatial distribution of stars is modelled using an exponential disk profile, which is a common representation of the Milky Way's disk [3]. The radial distances of the stars are drawn from an exponential distribution with a scale length of $R_d = 2.6\,\text{kpc}$ and the vertical distances are drawn from another exponential distribution with a scale height of $z_d = 0.3\,\text{kpc}$. The azimuthal angles are uniformly distributed between 0 and $2\pi$. The generated stars are plotted in Fig.1. This results in the position vectors being calculated as

$$\mathbf{r} = (R\cos(\phi), R\sin(\phi), z).$$

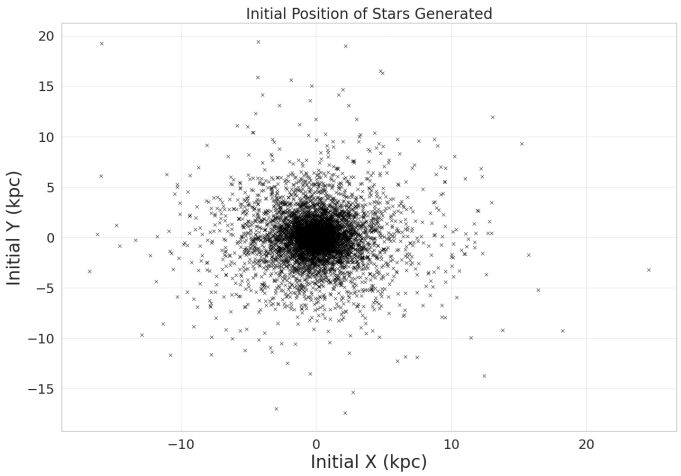


Figure 1: Initial positions of the generated stars in the simulation. The plot shows the distribution of stars in the X-Y plane, illustrating a central concentration typical of a galactic disc structure.

The velocities of the stars are initially set to match circular orbits around the galactic centre. The circular velocity at a given radius $R$ is calculated from the gravitational potential using the relation.

$$v_{\text{circ}} = \sqrt{R \cdot a_R},$$

where $a_R$ is the radial component of the acceleration due to the potential at radius $R$. The velocity vectors

are then set as

$$\mathbf{v} = (-v_{\text{circ}} \sin(\phi), v_{\text{circ}} \cos(\phi), 0),$$

ensuring that the stars follow circular orbits in the disk plane. The masses of the stars are generated according to the Kroupa Initial Mass Function (IMF), a broken power-law distribution commonly used to describe the distribution of stellar masses [16]. The IMF is defined by the following probability density function (PDF):

$$\xi(m) = \begin{cases} m^{-\alpha_1} & \text{if } m < m_{\text{break}} \\ m_{\text{break}}^{\alpha_2 - \alpha_1} m^{-\alpha_2} & \text{if } m \geq m_{\text{break}} \end{cases}$$

where $\alpha_1 = 1.3$ for masses below $m_{\text{break}} = 0.5\, M_\odot$ and $\alpha_2 = 2.3$ for masses above $m_{\text{break}}$. The function generates masses by drawing random values from this IMF's cumulative distribution function (CDF). Combining these elements, the function creates a population of stars with realistic spatial distribution, velocities, and masses based on the specified models and parameters. This provides a detailed and accurate initial setup for simulating the dynamics and evolution of stellar populations within the Milky Way's gravitational potential. The density function for the generated potential is plotted in Fig 2.

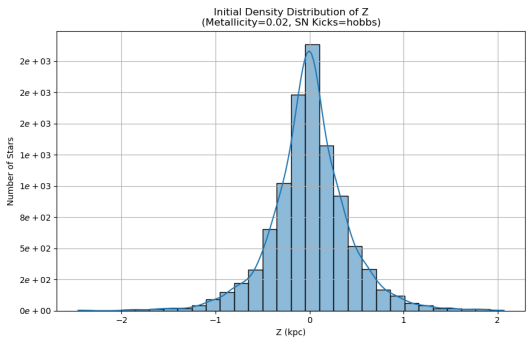


Figure 2: Initial density distribution of the Z positions of stars. The plot shows the number of stars as a function of their initial Z positions (kpc). The distribution is centered around Z = 0, indicating the stars are primarily located in the galactic plane initially.

## 2.4 Stellar Evolution

SEVN [14] is used to model the lifecycle of stars within a simulated galaxy. The process begins with generating initial masses using the Kroupa Initial Mass Function (IMF), which describes the distribution of stellar masses at birth. Stars are initialized with specific masses and metallicities, setting the stage for their subsequent evolution, which includes main sequence lifetimes, luminosities, and radii.During the simulation, stars evolve over discrete time steps. SEVNpy tracks changes in various stellar properties, such as mass loss due to stellar winds or binary interactions, luminosity changes, and stellar radius expansion. These updates are based on detailed stellar evolution models, incorporating various physical processes to simulate how stars evolve accurately. Massive stars can leave neutron stars and black holes behind during supernova explosions. These remnants can receive significant velocity kicks during the explosion, modelled in SEVNpy based on observational data and theoretical predictions. These velocity kicks are applied to the stars' velocities within the simulation, affecting their subsequent trajectories within the galaxy. This ensures that the dynamical effects of supernova explosions on stellar remnants are realistically represented. In addition to changes in position and velocity, stars also lose mass through winds or interactions. SEVNpy provides updated masses for the stars at each time step. The positions and velocities of stars are updated using a symplectic leapfrog integrator to ensure time-reversible updates and conserve energy over long simulations. This integrator calculates the new positions and velocities based on the gravitational acceleration from the galactic potential. SEVNpy continuously updates the stars' properties throughout the simulation, includes applying supernova kicks to remnants and updating masses based on stellar evolution models.

Our simulation investigated two configurations for supernova kicks. The first configuration, the Hobbs configuration, uses the Hobbs kick model, where the kicks are sampled from a Maxwellian distribution with a standard deviation of 265 km/s. The second configuration, the Hobbs Pure configuration, is

a variation of the Hobbs model with the same standard deviation but different assumptions about the kick velocity distribution. We considered two different metallicities for the stellar population for each kick model. The first metallicity, Solar Metallicity ($Z = 0.02$), represents a typical value for stars in the Milky Way. The second metallicity, Sub-solar Metallicity ($Z = 0.002$), represents a lower metallicity environment, typical for older stars or stars in the galaxy's outer regions.

# 3 Analysis

The comparison between Neutron Stars and Black Holes reveals several key differences in their distributions post-supernova. Initially, the stars concentrated near the galaxy's centre, with low cylindrical radii and Z positions. However, the final distributions show marked differences. Neutron Stars exhibit a broader spread in cylindrical radius and Z positions than Black Holes. This broader spread suggests Neutron Stars are more affected by the dynamics of supernova kicks than Black Holes. Specifically, Neutron Stars end up distributed over a wider range of cylindrical radii, indicating they are kicked further out from their initial positions. Additionally, the final Z positions of Neutron Stars display a greater vertical spread, suggesting higher kick velocities or more frequent kicks compared to Black Holes, which remain closer to the midplane of the galaxy. The impact of supernova kicks and metallicity further elucidates these differences. In scenarios with stronger or more frequent supernova kicks, Neutron Stars and Black Holes are more widely distributed, but Neutron Stars show a greater relative increase in spread. Conversely, in scenarios with weaker or less frequent kicks, the distributions remain closer to their initial states, with Neutron Stars still showing a slightly broader spread than Black Holes. Higher metallicity results in a more concentrated final distribution for both types of objects, though Neutron Stars continue to have a broader spread. Lower metallicity leads to a broader final distribution for both, with Neutron Stars displaying a more significant spread again. The histograms in Fig 6 and Fig 7 depict the initial and final Z positions and cylindrical radii of neutron star progenitors and black hole progenitors under varying metallicity and supernova kick model configurations. For the Z positions, stars with higher metallicity (0.02) and Hobbs kicks exhibit both progenitor types and display a wider spread post-supernova, indicating significant displacement due to supernova kicks. In lower metallicity (0.002), the final Z positions further widen, showing more significant displacement. Different kick models (Hobbs and Hobbs_pure) also impact the spread, with Hobbs_pure generally causing less pronounced displacement. The cylindrical radius analysis reveals that initially, stars cluster at low radii (0–2 kpc). After supernova events, the distributions broaden significantly, especially under lower metallicity, as stars are displaced to higher radii. The Hobbs model typically results in greater displacement compared to Hobbs_pure. Overall, supernovae and the associated kick velocities markedly redistribute stars, with lower metallicity and Hobbs kicks leading to more extensive spread.

# 4 Conclusion and Extention

Neutron Stars are more dynamically affected by supernova kicks than Black Holes, resulting in a broader radial and vertical distribution. Black Holes remain more concentrated towards the center and the galaxy's midplane. These differences highlight the distinct dynamical impacts supernova kicks have on Neutron Stars versus Black Holes, influenced by factors such as metallicity and the nature of the supernova kicks.

Future works could incorporate different Velocity dispersion, metalicities and natal kicks and extend it to binary objects to have a much more comprehensive understanding of these factors' influence the overall galactic evolution.

# References

[1] J. J. Andrews and V. Kalogera. The role of natal kicks in the formation of stellar-mass black hole

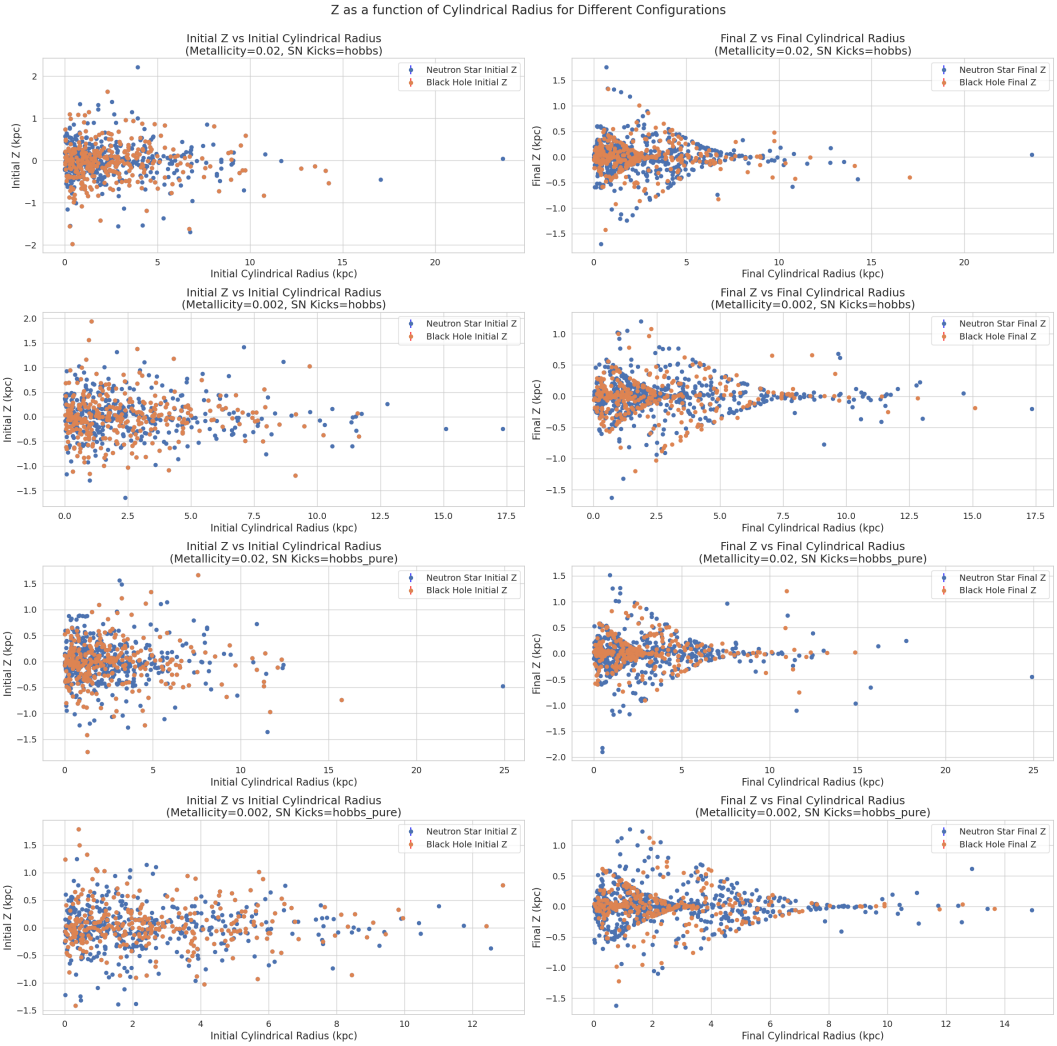


Figure 3: This figure illustrates the relationship between the Z position (in kpc) and the cylindrical radius (in kpc) for neutron stars and black holes, grouped by different configurations of metallicity and supernova (SN) kicks. The data is presented in six scatter plots organized in three rows, each corresponding to a unique configuration of metallicity and SN kicks. The top row represents Metallicity = 0.02, SN Kicks = hobbs; the middle row represents Metallicity = 0.002, SN Kicks = hobbs; and the bottom row represents Metallicity = 0.02 and 0.002, SN Kicks = hobbs_pure. In each subplot, blue points represent neutron stars and red points represent black holes. The left column shows the initial Z positions against the initial cylindrical radii, and the right column shows the final Z positions against the final cylindrical radii. The plots provide a visual comparison of how the positions of these stellar remnants change over time.

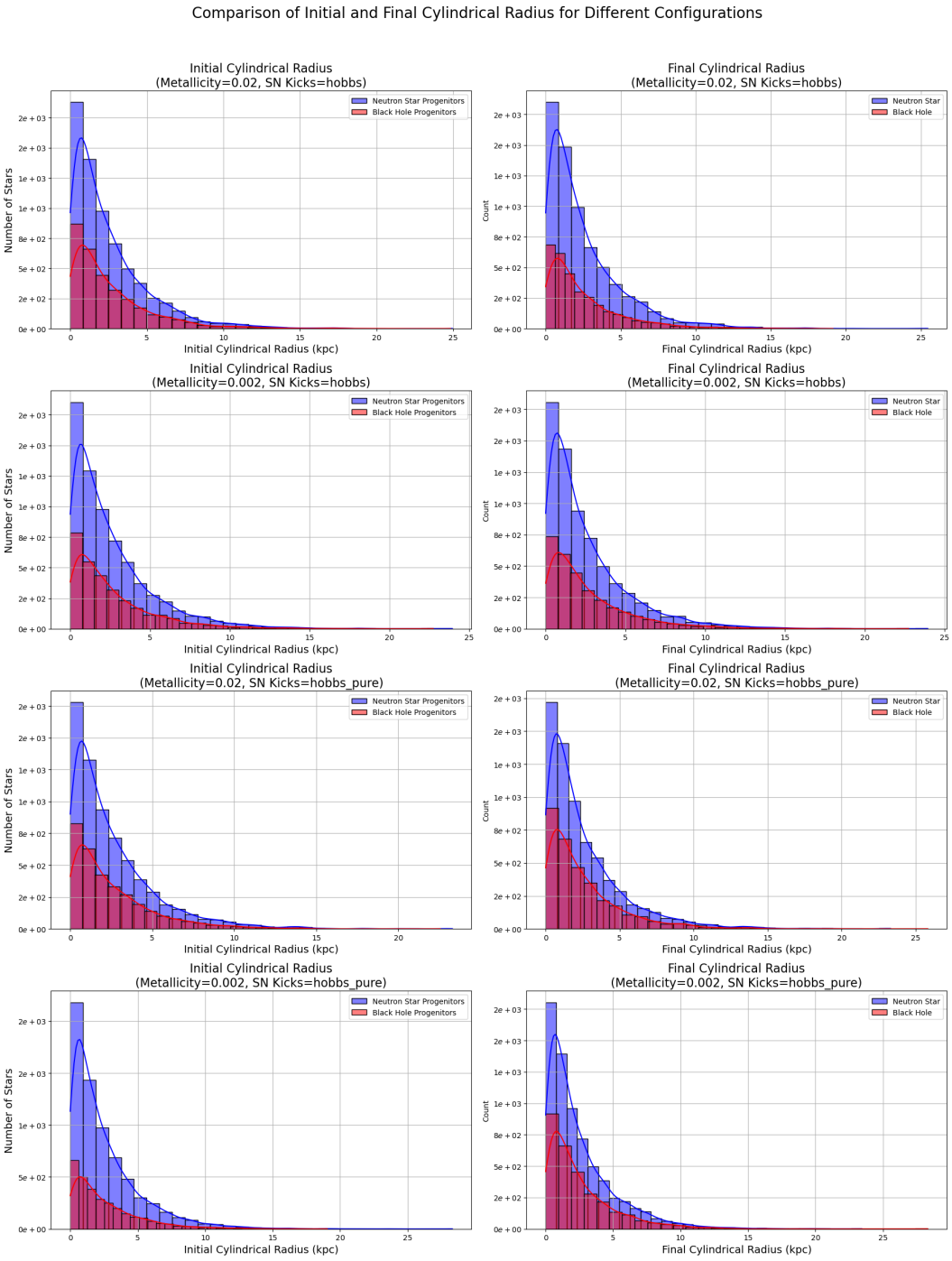


Figure 4: Comparison of initial and final cylindrical radii for different configurations. The top row shows initial and final cylindrical radii for stars with the Hobbs kick model and metallicities 0.02 and 0.002. The bottom row shows initial and final cylindrical radii for stars with the Hobbs_pure kick model and metallicities 0.02 and 0.002. Initial cylindrical radii are shown in the left column, while final cylindrical radii are shown in the right column. Neutron star progenitors and neuton stars are represented in blue, and black hole progenitors and black holes are represented in red.

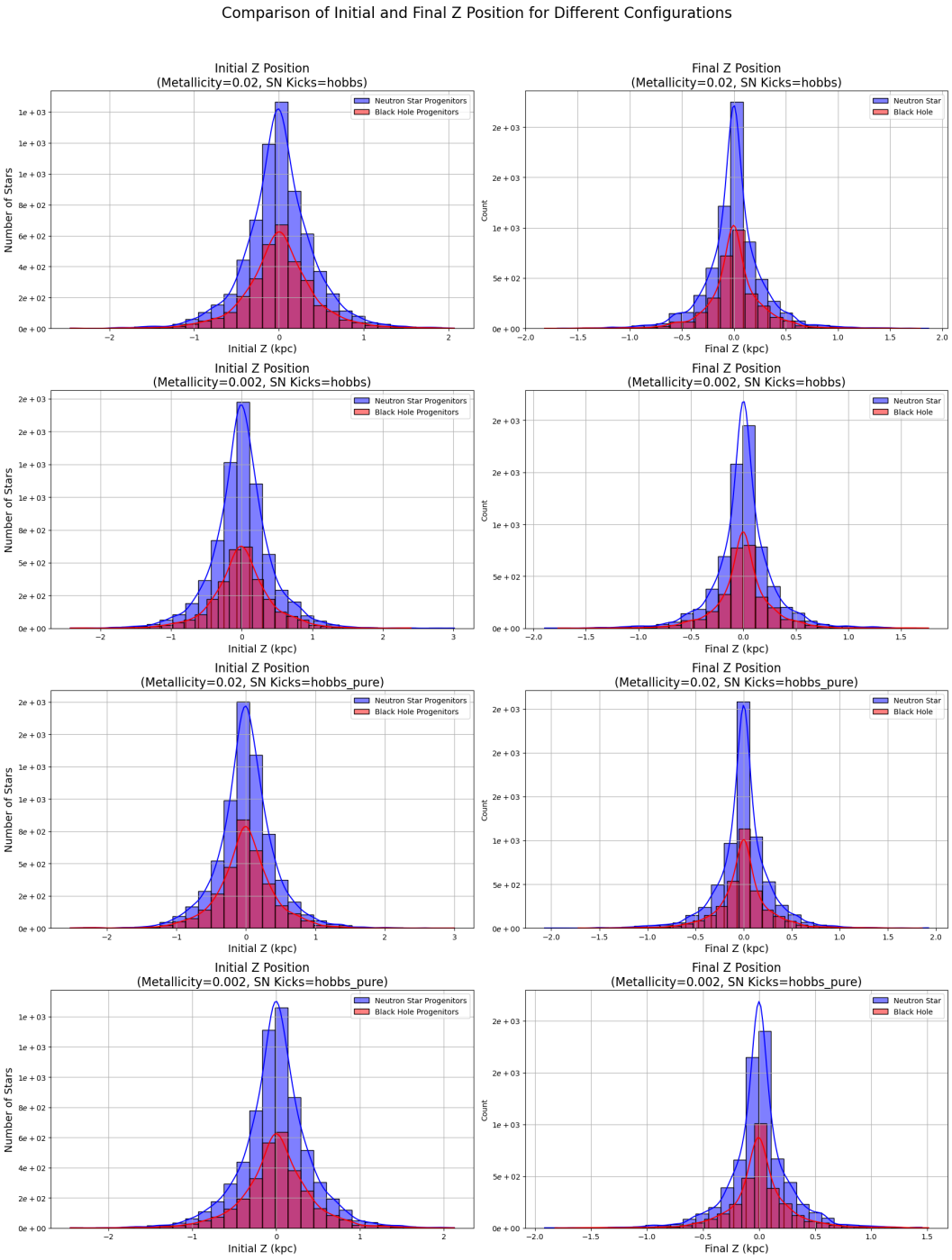


Figure 5: Comparison of initial and final Z positions for different configurations. The top row shows initial and final Z positions for stars with the Hobbs kick model and metallicities 0.02 and 0.002. The bottom row shows initial and final Z positions for stars with the Hobbs_pure kick model and metallicities 0.02 and 0.002. Initial Z positions are shown in the left column, while final Z positions are shown in the right column. Neutron star progenitors are represented in blue, and black hole progenitors are represented in red.

binaries. *The Astrophysical Journal*, 925:L1, 2022.

[2] et al. Atri, P. On the spins of stellar-mass black holes forming in massive star binaries. *The Astrophysical Journal*, 873:4, 2019.

[3] J. Binney and M. Merrifield. *Galactic Astronomy*. Princeton University Press, 1998.

[4] A. Blaauw. On the origin of the o- and b-type stars with high velocities (the "run-away" stars), and some related problems. *Bulletin of the Astronomical Institutes of the Netherlands*, 15:265, 1961.

[5] N. Brandt and P. Podsiadlowski. The effects of high-velocity supernova kicks on the orbital properties and sky distributions of neutron-star binaries. *Monthly Notices of the Royal Astronomical Society*, 274:461–484, 1995.

[6] J. M. Cordes and D. F. Chernoff. Neutron star population dynamics. ii. three-dimensional space velocities of young pulsars. *The Astrophysical Journal*, 505:315–338, 1998.

[7] J. M. Cordes, R. W. Romani, and S. C. Lundgren. Proper motion studies of pulsars. *Journal Name*, Volume Number:Page Numbers, 1993.

[8] et al. Fortin, M. Binary evolution and the properties of double neutron stars. *The Astrophysical Journal*, 925:87, 2022.

[9] T. et al. Fragos. Formation of black hole binaries in the galactic field. *The Astrophysical Journal*, 702:L143–L147, 2009.

[10] et al. Gandhi, R. Neutron star natal kicks and the spin-kick correlation. *Monthly Notices of the Royal Astronomical Society*, 485:594–608, 2019.

[11] J. E. Gunn and J. P. Ostriker. On the nature of pulsars. iii. analysis of observations. *The Astrophysical Journal*, 160:979–1002, 1970.

[12] L. Hernquist. An analytical model for spherical galaxies and bulges. *The Astrophysical Journal*, 356:359, 1990.

[13] J. G. Hills. The effects of sudden mass loss and a random kick velocity produced in a supernova explosion on the dynamics of a binary star of arbitrary orbital eccentricity - applications to x-ray binaries and to the binary pulsars. *The Astrophysical Journal*, 267:322–333, 1983.

[14] Giuliano Iorio, Michela Mapelli, Guglielmo Costa, Mario Spera, Gastón J. Escobar, Cecilia Sgalletta, Alessandro A. Trani, Erika Korb, Filippo Santoliquido, Marco Dall'Amico, Nicola Gaspari, and Alessandro Bressan. Compact object mergers: exploring uncertainties from stellar and binary evolution with SEVN. 2022. Publisher: arXiv Version Number: 5.

[15] P. G. Jonker and G. Nelemans. The galactic distribution of low-mass x-ray binaries and implications for their formation. *Monthly Notices of the Royal Astronomical Society*, 354:355–366, 2004.

[16] P. Kroupa. On the variation of the initial mass function. *Monthly Notices of the Royal Astronomical Society*, 322:231–246, 2001.

[17] A. G. Lyne and D. R. Lorimer. High birth velocities of radio pulsars. *Nature*, 369:127–129, 1994.

[18] I. Mandel. The orbital circularization of close double neutron stars by tidal interactions. *Monthly Notices of the Royal Astronomical Society*, 456:578–584, 2016.

[19] M. Miyamoto and R. Nagai. Three-dimensional models for the distribution of mass in galaxies. *Publications of the Astronomical Society of Japan*, 27:533, 1975.

[20] J. F. Navarro, C. S. Frenk, and S. D. M. White. The structure of cold dark matter halos. *The Astrophysical Journal*, 462:563, 1996.

[21] F. Özel, D. Psaltis, R. Narayan, and J. E. McClintock. The black hole mass distribution in the galaxy. *Journal Name*, Volume Number:Page Numbers, 2010.

[22] Davies M. B. Repetto, S. and S. Sigurdsson. Investigating stellar-mass black hole kicks. *Monthly Notices of the Royal Astronomical Society*, 425:2799–2809, 2012.

[23] E. P. J. Van den Heuvel, S. F. Portegies Zwart, D. Bhattacharya, and L. Kaper. Explaining the kicks and the space velocities of neutron stars. *The Astrophysical Journal*, 528:368, 2000.

[24] et al. Willems, B. The origin of the black hole binary gro j1655-40. *The Astrophysical Journal*, 616:414–430, 2004.

[25] et al. Zhang, B. Black hole kicks and their implications for double black hole mergers. *The Astrophysical Journal*, 773:87, 2013.

[26] et al. Zhao, R. Impact of supernova kicks on the survival of black hole x-ray binaries in the milky way. *Monthly Notices of the Royal Astronomical Society*, 518:L83–L88, 2023.